



## A new fluorescent H<sup>+</sup> sensor based on core-substituted naphthalene diimide

Rosalind P. Cox, Heather F. Higginbotham, Brenton A. Graystone, Saman Sandanayake, Steven J. Langford, Toby D.M. Bell\*

School of Chemistry, Monash University, Clayton, Victoria 3800, Australia

### ARTICLE INFO

#### Article history:

Received 13 September 2011

In final form 10 November 2011

Available online 19 November 2011

### ABSTRACT

The synthesis and spectroscopic characterisation of a new amino core-substituted naphthalene diimide is reported. The compound exhibits H<sup>+</sup> sensing properties leading to a change in optical output through both absorption and emission. On addition of trifluoroacetic acid, an increase in the fluorescence quantum yield from 0.5 to 0.67 and a ~500–550 cm<sup>-1</sup> blue shift of absorption and emission maxima are observed. Addition of triethylamine fully reverses these effects and the cycle is repeatable many times. The increase in fluorescence emission is attributed to protonation blocking weakly competitive photoinduced electron transfer operative in the neutral form of the molecule.

© 2011 Elsevier B.V. All rights reserved.

### 1. Introduction

Fluorescent chemosensors have been widely reported because of the advantages they possess over non-fluorescent chemosensors such as high sensitivity, real-time visualisation and a rapid response time [1]. Observable changes in absorption or fluorescence (or both) at a particular wavelength based on one or more inputs (protonic, ionic, electronic) has led to the development of commercial sensors and has contributed to the more futuristic area of molecular logic [2–4]. Fluorescent pH sensors have been especially useful in the areas of biology, medicine and the environment [5]. For example, changes in intracellular pH (pH<sub>i</sub>) are important in a number of biochemical processes and in determining disease states. There are two broad methods of studying pH<sub>i</sub> using ion-sensitive microelectrodes and dyes [6]. Fluorescent pH-sensitive dyes, e.g. fluoresceins, xanthenes and pyrenes have a range of different properties including pK<sub>a</sub>, excitation and emission wavelengths, lipid solubility, and photostability making them suitable for various applications. Naturally, the use of dyes to measure pH<sub>i</sub> is strongly influenced by the ability of target cells to retain the dye and that measuring pH is strongly affected by temperature, cell type, indicator dye and use of transport inhibitors to prevent dye export [7]. Hence new dye systems capable of systematic change of properties through functionalisation are always in need.

Naphthalene diimides (NDIs) are particularly desirable sensor candidates because they are small, easily functionalisable molecules with relatively broad solubility in a range of solvents and tunable fluorescent properties [8–13]. Although NDIs themselves have very weak emissions, core substituted NDIs (cNDIs) are able to fluoresce, especially with the introduction of electron donor

groups such as alkyl amines [14–16]. Substituted amino-NDIs (SANDIs) have strong photoluminescence and are brightly coloured, ranging from red through to blue [17]. Additionally, changing the substituents of a cNDI can greatly affect the absorbance and fluorescence of the NDI [5,7] allowing good, measurable photo-physical changes as required for an effective sensor. In recent work [18], a DBU-annulated SANDI exhibited changes in both absorbance and fluorescence in different pH environments which were attributed to internal charge transfer (ICT). Incorporation of additional amine groups in the substituents offers a way for the molecule to respond to environmental changes, particularly pH, whilst retaining the key features of the alkylated NDI system. With this in mind, we developed **1** with side groups containing two amine groups.

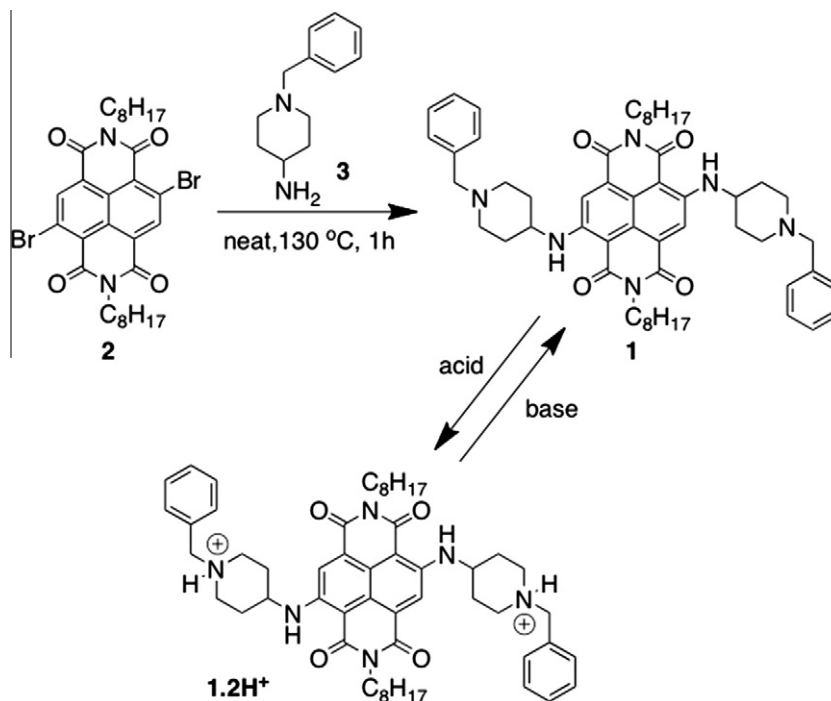
Many chemosensors operate using one of two basic systems: internal charge transfer (ICT) and photoinduced electron transfer (PET) [1]. Chemosensors designed for PET processes involve a fluorophore–spacer–receptor system that contains a PET acceptor (typically a fluorophore) and a PET donor (typically an amine) [19,20]. The PET process between *N,N*-disubstituted naphthalene diimide [21,22], naphthalimide [23–26] or related perylene diimide [27] based fluorophores have been studied [21] and PET has been reported in a SANDI based molecular system for sensing Zn<sup>2+</sup> [28]. Herein we report on the synthesis and spectroscopic analysis of a protic switch, disubstituted SANDI (DiSANDI) **1**, which exhibits PET properties and sensitivity to H<sup>+</sup> in both chloroform and toluene.

### 2. Materials and methods

The synthesis of the dark blue pH responsive compound **1** [29] was achieved (Scheme 1) by reacting *N,N*-bis(*n*-octyl)-2,6-dibromo naphthalene diimide **2** [30,31] with commercially available *N*-benzyl-4-aminopiperidine **3** under relatively mild conditions and stan-

\* Corresponding author. Fax: +61 3 9905 4597.

E-mail address: [toby.bell@monash.edu](mailto:toby.bell@monash.edu) (T.D.M. Bell).



**Scheme 1.** Synthesis of  $H^+$  responsive compound **1**, and the resultant compound **1.2H<sup>+</sup>** following protonation at the N atom in the piperidine ring of each core substituent.

standard work-up and purification procedures. As is also shown in [Scheme 1](#), compound **1** is able to accept a proton at the each of the piperyl N atoms in the side groups (see below) and this form of the molecule is referred to as **1.2H<sup>+</sup>**. Full synthetic details are given in the Supplementary Material along with characterisation spectra in [Figures S9–16](#).

UV–Vis spectra were obtained using a Varian Cary 100 Bio UV–Visible Spectrophotometer. Emission spectra were recorded using a Varian Cary Eclipse fluorescence spectrophotometer in 1 cm quartz cuvettes. Acidification and basification in chloroform (Aldrich, spectroscopic grade) was achieved by adding aliquots of trifluoroacetic acid (TFA, 0.6 mM, 20  $\mu$ L, Aldrich AR grade) and triethylamine (TEA, 0.7 mM, 40  $\mu$ L, Aldrich AR grade), respectively, to a solution of **1** (2.5 mL). Fluorescence quantum yields were determined by comparing areas under corrected emission spectra recorded under identical conditions with that of Rhodamine 101 ( $\Phi_f = 1.00$  in 0.01% HCl in EtOH [32] (Aldrich spectroscopic grade)). Solutions of Rhodamine 101, **1** and **1.2H<sup>+</sup>** were prepared in quartz cuvettes, with their absorbance at 550 nm being less than 0.1 in order to avoid inner filter effects. They were deoxygenated by bubbling with  $N_2$  gas for 20 min immediately prior to measurement. Corrections were made for the different refractive indexes of the solvents and for any differences in the fraction of light absorbed at the excitation wavelength.

Fluorescence decay histograms were obtained using the method of Time Correlated Single Photon Counting (TCSPC) with excitation from a picosecond pulsed supercontinuum fiber laser (Fianium, SC 400-4-pp) providing  $\sim 40$  ps pulses across the visible and near IR at 5 MHz repetition rate. Excitation wavelength selection was achieved using a 700 nm shortpass filter and 10 nm bandpass filter centred at 594 nm (Chroma). Emission from the sample was collected at  $90^\circ$  to excitation and passed through a monochromator (CVI, dk480) and focused onto a fast response avalanche photodiode detector (APD, Id-Quantique, Id-100). Photon emission times were recorded by a photon counting module (Picoquant, PicoHarp 300) with start signal provided by a sync out from the excitation laser and stop signal from the APD detector. An instrument response function (IRF) recorded from a scattering solution (dilute milk powder in

water) had a full width half maximum of  $\sim 90$  ps. Prior to measurement all samples were degassed either through several freeze–pump–thaw cycles or by bubbling with nitrogen for 20 min immediately before measurement. Fluorescence decay times were obtained by fitting the data with a single exponential decay function convolved with the IRF using an iterative least-squares routine based on the Levenberg–Marquardt algorithm. Goodness of fit was judged by the chi-squared parameter ( $\chi^2$ ) and by inspection of the residuals. Decay histograms and fit functions are given in the [Supporting Information](#).

### 3. Results and discussion

UV–Vis absorption spectra of **1** in  $CHCl_3$  ( $[1] = 10 \mu M$ ) with varying amounts of trifluoroacetic acid (TFA) are shown in [Figure 1](#). The spectrum in neat  $CHCl_3$  shows characteristic peaks between 330 and 400 nm corresponding to the  $\pi$ – $\pi^*$  transitions of the NDI

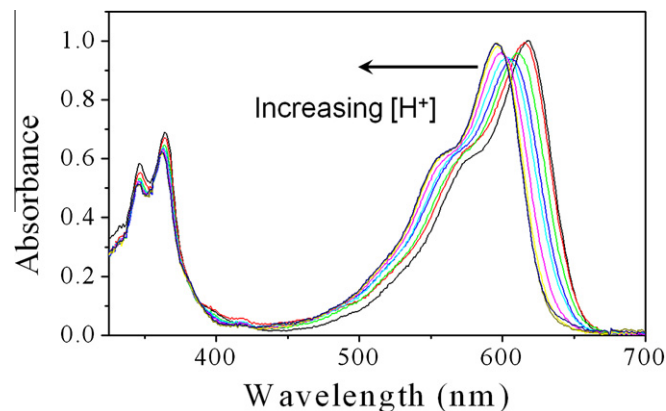


**Figure 1.** Normalised UV–Vis absorption spectra of **1** in  $CHCl_3$  ( $[1] = 10 \mu M$ ) with different concentrations of TFA ( $[TFA] = 0, 2.5, 5.0, 7.5, 10, 12.5, 15, 17.5, 20 \mu M$ ).

core. A strong, broad absorption at a longer wavelength is also present with a maximum at 618 nm and a molar absorption coefficient of  $16700 \text{ M}^{-1} \text{ cm}^{-1}$  at this wavelength (See Figure S1 in the Supplementary Material). This band is characteristic of  $n-\pi^*$  transitions made available by donation of electron density into the NDI core primarily from the lone pairs on the N atoms immediately adjacent to the NDI core [23]. Upon addition of TFA, the major absorption peak at 618 nm begins to blue shift (Figure 1, spectra where  $[\text{TFA}] = 2.5, 5.0, 7.5, 10, 12.5, 15, 17.5, 20 \mu\text{M}$ ) ultimately by  $515 \text{ cm}^{-1}$  to 598 nm ( $[\text{TFA}] = 20 \mu\text{M}$ ) with no significant change in absorptivity. The addition of acid does not alter the NDI peaks between 330 and 400 nm, implying that the protonation does not affect transitions relating to the NDI core. Fluorescence excitation spectra of **1** and **1.2H<sup>+</sup>** are very similar in shape to their absorption spectra (see Figure S2 in the Supplementary Material).

Fluorescence emission spectrum of **1** in  $\text{CHCl}_3$  is shown in Figure 2 along with the titration of TFA to form **1.2H<sup>+</sup>**. Clearly evident is an increase in the total fluorescence with an unusual concomitant blue shift of 22 nm ( $549 \text{ cm}^{-1}$ ) in the maxima as a protic response [33]. The fluorescence quantum yields of the neutral and protonated species were calculated in  $\text{CHCl}_3$  to be 0.50 and 0.67, respectively, using Rhodamine 101 as a reference [32]. The stoichiometry of binding was determined from fluorescence titration data to be 1:2 (see Figure S3 in the Supplementary Material). Steady state UV–Vis and fluorescence spectra indicate that protonation occurs at both sites at essentially the same pH. This implies that addition of a proton at one site has negligible effect on the pKa of the other protonation site which is reasonable given their placement out on the side arms of the molecule.

The blue shift that arises from the protonation of **1** is unusual for a pH sensor [21,27] and is an advantageous property for such applications. Sensors with only an intensity change response need to be effectively 'ON-OFF' systems in order to provide a clear 'read-out'. A sensor showing a spectral shift enables a ratiometric approach to be taken by comparing the intensities at the respective maxima of the bound and free states. The difference of  $549 \text{ cm}^{-1}$  in the emission maxima and the change in quantum yield of the protonated and neutral forms of the molecule, yield an approximately eightfold emission output difference (for the same fraction of light absorbed) in the spectral region of 600–620 nm while still retaining 20% of the total emission output of the protonated system. An approximately  $8\times$  output change is not as pronounced as other PET based sensors,

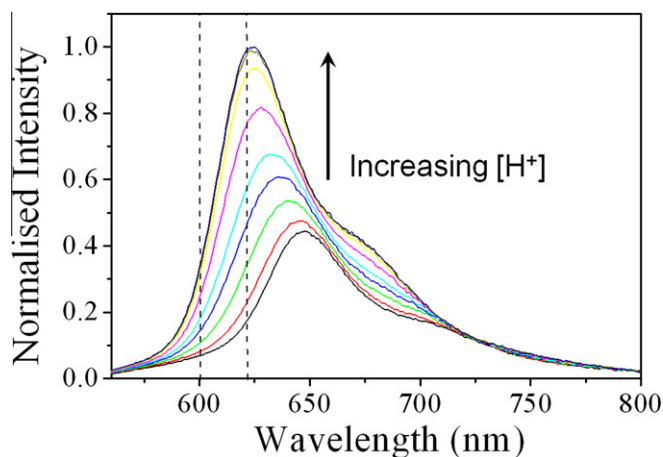


**Figure 2.** Corrected fluorescence emission spectra ( $\lambda_{\text{ex}} = 550 \text{ nm}$ ) of **1** in  $\text{CHCl}_3$  ( $[\mathbf{1}] = 10 \mu\text{M}$ ) with the different concentrations of TFA ( $[\text{TFA}] = 0, 2.5, 5.0, 7.5, 10, 12.5, 15, 17.5, 20 \mu\text{M}$ ). The vertical dashed lines are a guide to the eye indicating the region of greatest intensity difference for **1** and **1.2H<sup>+</sup>** (approximately eightfold when adjusted for the different fractions of light absorbed at the excitation wavelength).

**Table 1**  
Optical properties for **1** and **1.2H<sup>+</sup>** in  $\text{CHCl}_3$  and toluene.

DiSANDI	Solvent	$\lambda_{\text{abs}}$ [nm]	$\lambda_{\text{em}}$ [nm]	$\Phi_f$	$\tau_{\text{flu}}$ [ns]
<b>1</b>	$\text{CHCl}_3$	364, 618	644	0.50	10.2
<b>1.2H<sup>+</sup></b>	$\text{CHCl}_3$	363, 598	622	0.67	11.9
<b>1</b>	Toluene	365, 612	639	0.54	10.5
<b>1.2H<sup>+</sup></b>	Toluene	363, 593	619	0.70	11.3

e.g. those of Abad et al.  $\sim 12\times$  [23], Daffy et al.,  $\sim 12\times$  [24] and Zhou et al.,  $\sim 24\times$  [18], however, it could be useful, with appropriate thresholds, for pH sensor applications [34]. A possible advantage of the molecule having significant emission both when neutral and protonated, is that it can be used simply as a fluorescent label under a wide range of  $\text{H}^+$  concentrations.

The optical properties the protic response of **1** was also examined in toluene. The compound displays only very marginally blue-shifted ( $\sim 100 \text{ cm}^{-1}$ ) absorption and emission in the main transition in the visible spectrum and responds in a very similar fashion to the addition of TFA with an increase in fluorescence quantum yield from 0.54 to 0.70 and a blue shift of the emission of  $506 \text{ cm}^{-1}$ . This is probably a result of the molecule being highly symmetrical and change in solvent polarity has little effect on the dipole of the molecule in both neutral and protonated forms. Data for both solvents are given in Table 1.

The reversibility of the acid-induced fluorescence increase and blue shift were tested by deprotonating **1.2H<sup>+</sup>** through addition of triethylamine (TEA). Addition of TEA to **1.2H<sup>+</sup>** in  $\text{CHCl}_3$  led to a decrease in fluorescence and concomitant red shifting of the emission maximum back to 644 nm, implying a complete switching to **1**. Repeatability of the switching was tested by alternately adding TFA and TEA to **1** in  $\text{CHCl}_3$  over nine cycles as shown in Figure 3. Similar results were obtained in toluene. Control experiments using *N,N'*-(dibutyl)-2,6-(dibutylamino)-1,4,5,8-naphthalene diimide which contains simple alkylamino core substituents. No changes in absorption or emission of this compound on addition of TFA or TEA were observed indicating that the N atoms in the piperidine rings of **1** are the protonation sites.

Time-resolved fluorescence profiles were recorded by TCSPC for **1** and **1.2H<sup>+</sup>** in toluene and  $\text{CHCl}_3$ . Decay histograms could be well fitted in all cases by a single exponential decay function convolved with an instrument response function. TCSPS data and fitting de-

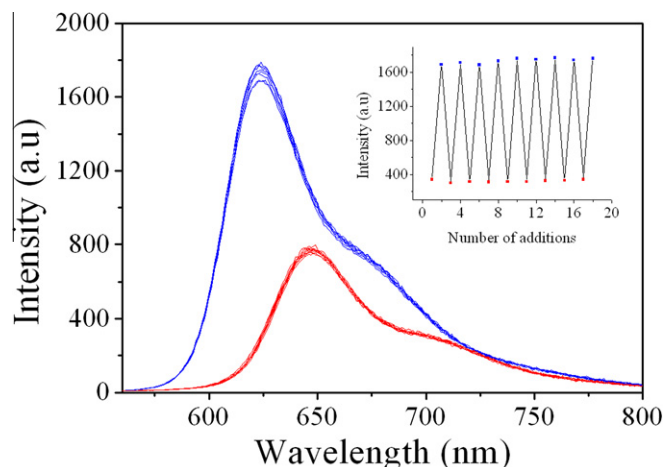


**Figure 3.** Fluorescence emission spectra of **1** and **1.2H<sup>+</sup>** in  $\text{CHCl}_3$  solution with alternating addition of TFA and TEA. Inset: Fluorescence intensity vs. number of additions at 622 nm ( $\lambda_{\text{ex}} = 550 \text{ nm}$ ). Note: the absorbance of **1.2H<sup>+</sup>** at 550 nm is approximately 1.6 times that of **1** in  $\text{CHCl}_3$ .

tails are included in the Supporting Information. Fluorescence lifetimes,  $\tau_{\text{flu}}$  (decay constant reciprocals) are given in Table 1 and are relatively long, ranging between 10 and 12 ns. Such lifetimes are similar to those of another di-allyl core substituted SANDI [13]. There is little variation with solvent, however the lifetime of **1** in both solvents is reduced by about 10–15% compared to **1.2H<sup>+</sup>** consistent with the reductions in QY also observed. These differences suggest the presence of a weakly competitive quenching mechanism operative in the neutral form of the molecule. Given the electron accepting properties of NDIs and electron donating properties of amines, this is attributable to photoinduced electron transfer (PET) from the piperidine on one of the core substituents to the NDI core. Protonation of the piperyl N atoms would block this mechanism, thus removing its quenching effect on QY and lifetime. PET has been observed in many systems, usually being far more efficient and leading to an 'ON-OFF' system [1].

The presence of PET can account for the differences in fluorescence lifetime and quantum yield of **1** and **1.2H<sup>+</sup>**, however, does not in itself, explain the blue shift on protonation. The origin of this shift may arise, however, as a result of protonation by causing the loss of a small amount of electron donation from the N atoms in the piperidine rings of the substituents into the NDI core. It is well established that the fluorescence band of SANDIs in the visible region is due to electron donation from N atoms immediately adjacent to the core [15] and that increasing the number of substituents on the core (hence the amount of electron donation into the core) leads to further red shifts, i.e.  $\lambda_{\text{em}} \text{ tetra} > \text{di} > \text{mono}$  [17]. The piperyl N atoms may contribute some additional electron density via overlap of their lone pair with that of the N atoms adjacent to the core adding to the red shift of the transition. This effect would be lost when the piperyl N atoms are protonated. Interaction between adjacent piperidine rings in a donor–acceptor triad system was previously seen by Brouwer et al. [35].

To investigate this possibility, the ground state geometry and HOMO orbitals of **1** and **1.2H<sup>+</sup>** in the gas phase were modelled at the B3LYP/6-31(d) level of theory [36] and are shown in Figure 4. The distance between the two nitrogen atoms in the side groups was found to be 4.1 Å. The lone pairs of the N atoms adjacent to the core are conjugated with the electron cloud of the NDI core

facilitated by the hydrogen bond between the amine hydrogen and the imide oxygen yielding a planar geometry. The lone pairs of the N atoms of the piperidine rings were found to be slightly angled towards the NDI core with a clear line of sight to the N atoms immediately adjacent to the core. There is a small but discernable (at 99% contour) amount of electron density in the HOMO of **1** present on the N atoms in the piperidine rings while none is seen for **1.2H<sup>+</sup>**. This suggests that additional electron donation from the piperyl N atoms into the core is possible for **1** and presumably this would lower the energy of the transition, red-shifting it. This effect would be lost on protonation thus the transition in **1.2H<sup>+</sup>** is blue-shifted with respect to **1**.

#### 4. Conclusion

The synthesis of a new SANDI derivate substituted with two core substituents each containing a piperidine ring has been achieved. The compound has been fully characterised and found to exhibit a reversible protic response through both colour and emission. There is an increase in fluorescence quantum yield and emission lifetime of 10–15% in the presence of H<sup>+</sup> which is accompanied by a blue-shift of  $\sim 500\text{--}550 \text{ cm}^{-1}$  in both absorption and emission maxima. These effects are fully reversible on addition of base and can be repeated many times. Protonation is occurring at piperyl N atoms and this blocks a weakly competitive PET process which leads to the emission increase. While the design is appropriate to exhibit control, future work will be aimed at making the system more optically sensitive to protonation and to diversify this research into the sensing of exogenous anions.

#### Acknowledgement

Financial support from the Australian Research Council through the Discovery Grant Scheme (DP1093337) is gratefully acknowledged.

#### Appendix A. Supplementary data

Supplementary data associated with this article can be found, in the online version, at doi:10.1016/j.cplett.2011.11.028.

#### References

- [1] N.I. Georgiev, V.B. Bojinov, *Dyes Pigm.* 84 (2010) 249.
- [2] A.P. de Silva et al., *J. Am. Chem. Soc.* 129 (2007) 3050.
- [3] A.P. de Silva, M.R. James, B.O.F. McKinney, D.A. Pears, S.M. Weir, *Nat. Mater.* 5 (2006) 787.
- [4] S.J. Langford, T. Yann, *J. Am. Chem. Soc.* 125 (2003) 11198.
- [5] Z.Z. Li, C.G. Niu, G.M. Zeng, Y.G. Liu, P.F. Gao, G.H. Huang, Y.A. Mao, *Sens. Actuators B* 114 (2006) 308.
- [6] A. Salvi, J.M. Quillan, W. Sadee, *AAPS PharmSci.* 4 (2002).
- [7] N.A. Ritucci, J.S. Erlichman, J.B. Dean, R.W. Putnam, *J. Neurosci. Methods* 68 (1996) 149.
- [8] S.V. Bhosale, S.V. Bhosale, M.B. Kalyankar, S.J. Langford, *Org. Lett.* 11 (2009) 5418.
- [9] S.V. Bhosale, C.H. Jani, S.J. Langford, *Chem. Soc. Rev.* 37 (2008) 331.
- [10] S.V. Bhosale, M.B. Kalyankar, S.V. Bhosale, S.J. Langford, E.F. Reid, C.F. Hogan, *New J. Chem.* 33 (2009) 2409.
- [11] D. Buckland, S.V. Bhosale, S.J. Langford, *Tet. Lett.* 52 (2011) 1990.
- [12] K.P. Ghiggino et al., *Adv. Funct. Mater.* 17 (2007) 805.
- [13] T.D.M. Bell et al., *Chem. – Asian J.* 4 (2009) 1542–1550.
- [14] N. Sakai, J. Mareda, E. Vauthey, S. Matile, *Chem. Commun.* 46 (2010) 4225.
- [15] C. Thalacker, C. Röger, F. Würthner, *J. Org. Chem.* 71 (2006) 8098.
- [16] F. Würthner, S. Ahmed, C. Thalacker, T. Debaerdemaeker, *Chem. – Eur. J.* 8 (2002) 4742.
- [17] R.S.K. Kishore et al., *J. Am. Chem. Soc.* 131 (2009) 11106.
- [18] C. Zhou, Y. Li, Y. Zhao, J. Zhang, W. Yang, Y. Li, *Org. Lett.* 13 (2010) 292.
- [19] R. Ameloot, M. Roeffaers, M. Baruah, G. De Cremer, B. Sels, D. De Vos, J. Hofkens, *Photochem. Photobiol.* 8 (2009) 453.
- [20] A.P. de Silva, J. Eilers, G. Zlokarnik, *Proc. Natl. Acad. Sci.* 96 (1999) 8336.
- [21] S. Alp, S. Erten, C. Karapire, B. Köz, A.O. Doroshenko, S. İçli, *J. Photochem. Photobiol. A Chem.* 135 (2000) 103.
- [22] S.J. Langford, M.J. Latter, C.P. Woodward, *Photochem. Photobiol.* 82 (2006) 1530.

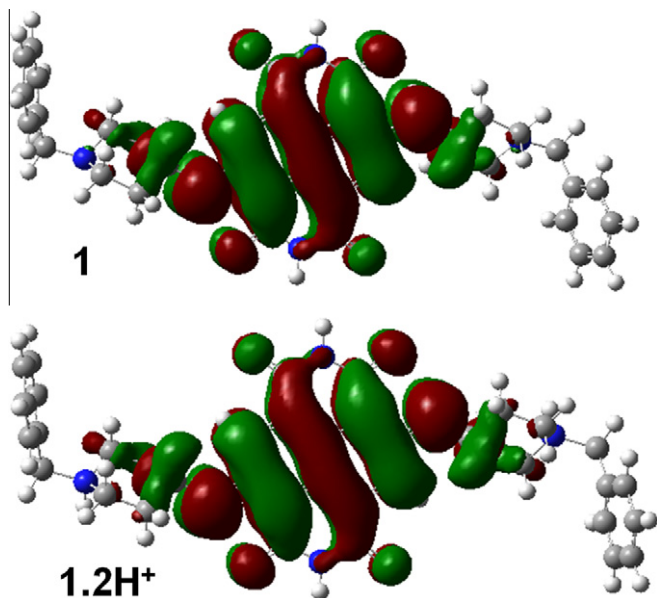


**Figure 4.** Ground state geometry of **1** (upper panel), and **1.2H<sup>+</sup>** (lower panel) with HOMO orbitals shown at 99% contour. There is a small amount of electron density is present on N atoms in piperidine rings for **1** which is not present for **1.2H<sup>+</sup>**.

- [23] S. Abad, M. Kluciar, M.A. Miranda, U. Pischel, *J. Org. Chem.* 70 (2005) 10565.
- [24] L.M. Daffy, A.P. de Silva, H.Q.N. Gunaratne, C. Huber, P.L.M. Lynch, T. Werner, O.S. Wolfbeis, *Chem. – Eur. J.* 4 (1998) 1810.
- [25] L. Shen, X. Lu, H. Tian, W. Zhu, *Macromolecules* 44 (2011) 5612.
- [26] H. Wang, H. Wu, L. Xue, Y. Shi, X. Li, *Org. Biomol. Chem.* 9 (2011) 5436.
- [27] L. Zang, R. Liu, M.W. Holman, K.T. Nguyen, D.M. Adams, *J. Am. Chem. Soc.* 124 (2002) 10640.
- [28] X.Y. Lu, W.H. Zhu, Y.S. Xie, X. Li, Y.A. Gao, F.Y. Li, H. Tian, *Chem. – Eur. J.* 16 (2010) 8355.
- [29] Compound 1 was formed in 69% yield. <sup>1</sup>H NMR (300 MHz, 300 K): 9.45 (d, 5.7 Hz, 1H, NH), 8.10 (s, 2H, ArH), 7.2–7.4 (m, 10H, ArH), 4.14 (t, 5.7 Hz, 4H, NCH<sub>2</sub>), 3.69 (m, 2H, NHCH), 3.57 (s, 4H, CH<sub>2</sub>Ar), 2.89 (m, 4H), 2.30 (t, 4H), 2.12 (m, 4H), 1.7 (m, 8H), 1.2–1.5 (m, 20H), 0.8 (m, 6H). <sup>13</sup>C NMR (100 MHz, CDCl<sub>3</sub>, 300 K): 166.48, 163.42, 148.59, 129.43, 128.60, 127.42, 126.12, 121.59, 118.79, 102.35, 63.38, 52.25, 40.84, 40.06, 32.76, 32.18, 32.12, 29.99, 29.69, 29.59, 29.58, 29.53, 28.47, 27.57, 27.27, 23.70, 22.98, 22.96, 14.42, 14.40. ESMS *m/z* calcd for C<sub>54</sub>H<sub>71</sub>N<sub>6</sub>O<sub>4</sub> 867.5530, found 867.5530.
- [30] F. Chaignon, M. Falkenstrom, S. Karlsson, E. Blart, F. Odobel, L. Hammarstrom, *Chem. Commun.*, (2007) 64–66.
- [31] X. Gao et al., *Org. Lett.* 9 (2007) 3917.
- [32] T. Karstens, K. Kobs, *J. Phys. Chem.* 84 (1980) 1871.
- [33] R. Bissell, A. Prasanna de Silva, H. Nimal Gunaratne, P. Mark Lynch, G. Maguire, C. McCoy, K. Samankumara Sandanayake, *Fluorescent PET (photoinduced electron transfer) sensors*, in: J. Mattay (Ed.), *Photoinduced Electron Transfer V*, Springer, Berlin/Heidelberg, 1993, pp. 223–264.
- [34] The inset to Figure 3 shows the intensity at 625 nm varying repeatably over a 5-fold range. The greatest intensity ratio was found to be at 605 nm with a fluorescence intensity of the protonated form 15 times greater than the neutral form.
- [35] R.J. Willemsse, J.J. Piet, J.M. Warman, F. Hartl, J.W. Verhoeven, A.M. Brouwer, *J. Am. Chem. Soc.* 122 (2000) 3721.
- [36] M.J. Frisch et al., R.A. GAUSSIAN 09, GAUSSIAN, Inc., Wallingford CT, 2009.